EARTHQUAKE ENGINEERING AND STRUCTURAL DYNAMICS, VOL. 27, 67–90 (1998)

SHAKING TABLE TESTS ON 24 SIMPLE MASONRY BUILDINGS

D. BENEDETTI*[1], P. CARYDIS[2] AND P. PEZZOLI[3]

[1]*Department of Structural Engineering, Politecnico di Milano 32, I-20133 Milano, Italy*
[2]*LEE, NTUA, Athens*
[3]*ISMES, Bergamo*

Dedicated to professor Franz Ziegler, Vienna University for Technology

SUMMARY

The paper presents the results of a large experimental programme carried out on models, scaled 1:2, of two-storey masonry buildings. After suffering damage, the models were repaired and strengthened and tested again. A total of 24 buildings were subjected to 119 shaking-table tests, by ISMES (Italy) and LEE (Greece) facilities. The results allow to assess the efficiency of the various strengthening techniques employed and to describe the change of dynamic properties of the systems at the increase of damage. © 1998 John Wiley & Sons, Ltd.

Earthquake Engng. Struct. Dyn., **27**, 67–90 (1998)

KEY WORDS: masonry; shaking table; retrofitting; modal parameters

1. INTRODUCTION

Over the last two years, the Commission of the European Community (CEC) has funded, within the Environment Project, an experimental research aimed at better understanding the seismic behaviour of existing masonry buildings, generally non-engineered or not designed with reference to any code, and at analysing the efficiency of different techniques to improve it, both as prior-strengthening interventions and as repair methods after damage. Tests were carried out on models scaled 1:2 with ISMES (Seriate, BG, Italy) and LEE (Laboratory for Earthquake Engineering, NTUA, Athens, Greece) shaking-table facilities. A total of 14 models were built (8 in Italy and 6 in Greece). After suffering severe damage, the models were repaired and tested again. Twenty-four shaking-table testing sequences (each consisting of 4–7 shocks for ISMES tests and 2–6 for LEE ones) were carried out. To simulate real earthquakes, three-component base excitations were used for each shock. Several, though simple, geometric configurations were considered. Two material types and various retrofitting methods were taken into account. These features differentiate this experimental research from previous ones carried out with similar targets in various countries (U.S.A., Mexico, Peru, Italy, Slovenia, India, etc.), which are in fact limited to one or two models, often using a small length scale and a single-component base input. The analysis of the large amount of data obtained during the 119 shaking-table tests, improves the knowledge about response mechanisms of masonry buildings under seismic actions and about the change of their mechanical and dynamic properties as damage increases. Moreover, the results enable us to propose a hierarchy of the efficiency of retrofitting methods, to compare the observed behaviour to that predicted by analytical and design methods, to develop structural identification procedures from

* Correspondence to: Duilio Benedetti, Department of Structural Engineering, Politecnico di Milano, Piazza Leonardo da Vinci 32, I-20133 Milano, Italy

Contract grant sponsor: European Community; Contract grant number: EV5V-CT92-0174

CCC 0098–8847/98/010067–24$17·50

Received 1 July 1996
Revised 1 April 1997

seismic records or to check existing ones, to assess code prescriptions (e.g. related to the lateral force coefficient and to the reduction factor), to attempt diagnostic procedures based on dynamic responses. Most of these items are dealt with in References 1–3, but only some of them, described in Section 4, will be discussed in this paper, due to space limitations. Here we present the main results and their interpretation: data and results are available on request to perform further analyses on a cooperative basis.

2. MODELS AND SIMULATED BUILDINGS

2.1. Laws of similitude

The models are intended to represent elementary buildings in Mediterranean seismic prone areas. Figure 1 shows their basic configuration and Figure 2 three brick-masonry models, built at ISMES, after repair. In Figure 1 the dimensions of the models (in parentheses) and of the simulated buildings are shown in cm. The models were built with a length scale $S_L = 1/2$, to allow the use of the same materials as in the simulated structures. The acceleration and the stress scales were, respectively, $S_a = 1$ and $S_\sigma = 1$, since both systems are subjected to gravity acceleration and since the same material properties hold for models and real systems. According to the theory of models, the complete dynamic similitude leads to the following scales: force scale $S_F = 1/4$, velocity and time scales $S_v = S_t = 1/\sqrt{2}$, frequency scale $S_f = \sqrt{2}$, density scale $S_\rho = 2$. Since the same material was used for models and real buildings, additional masses were applied to the model to respect this scale. The total mass of the models ranges from 8 to 9 t, depending on the material type. Additional masses (of the same order of magnitude) were placed on the slabs (about 70 per cent) and distributed (30 per cent) over the walls of the two storeys. Details of these arrangements are reported in References 2 and 3. Concentrating additional masses at the slab levels of the models causes a mass distribution which is different from the one occurring in real systems, where masses are mainly due to walls and can hence be considered as roughly uniformly distributed along the height of the building. Additional masses on slabs produce a response mechanism in the model which differs from the real one: as known, when the same material is used, this difference becomes more significant as the length scale decreases. This fact is an intrinsic limitation of dynamic model testing; in the present case it is bounded by the relatively high length scale S_L. The observed performance of the model during a given shock is, however, worse than that of the real building, due to the additional masses at the slab levels. In our case it may be estimated that the state of stress at the bases of resisting walls during a shock is 10–15% higher in the model than in the simulated building. Input and output signals, recorded during the tests, refer to the scales stated above (for instance, to a compressed scale for time). However, the laws of similitude allow to refer all quantities of interest to the simulated (real) building. Hence, in what follows, all data, signals, results and the relevant discussion always refer to the 1:1 scale and to the real building.

2.2. Configurations and material properties

Only response accelerations were recorded, their locations are shown in Figure 1. Walls parallel to the x-axis or to the y-axis will be referred to what follows as x-walls or y-walls. The north side of the building is defined by y-walls opposite to the door openings of x-walls. Despite their simplicity, the models reproduce two items that may be critical during the response to a strong earthquake in existing masonry buildings. These are: (a) the connection along vertical edges between orthogonal walls and (b) the connection of slabs to the supporting walls. The basic geometrical configuration of Figure 1 was not kept constant for all the models, as far as the windows of y-walls are concerned. In configuration c1 there were windows in both storeys in both N and S y-walls, in configuration c2 there were windows in both storeys only in N walls while in configuration c3 they existed, still at both levels, only in S walls. Models built in Greece had arches spanning the openings (see Figure 3), to be consistent with the building technology used in the area. Seven models were built of bricks (Br) and seven of roughly squared stones (St). In all buildings the wall thickness

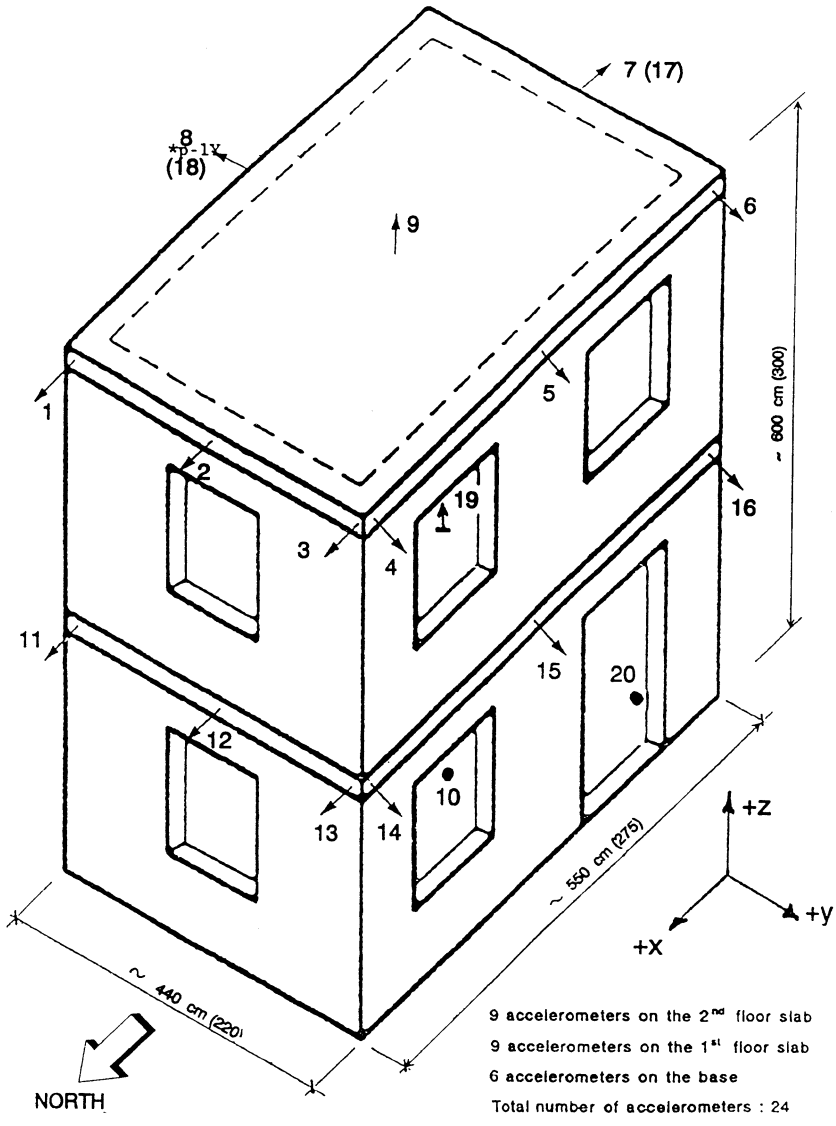

Figure 1. Basic configuration of the buildings and locations of measurement points

(at the real scale) is 45 cm. The mortar is deliberately of poor quality, reproducing the bad conditions of real existing buildings. Brick and stone wall panels were built and tested to obtain the masonry compression and diagonal tensile strengths. The average values of such strengths are reported in Table I with the compression strength of the mortar.

Stone-masonry systems built at ISMES were deliberately of very poor quality construction (e.g. no care in connecting orthogonal walls) to simulate the situation in existing buildings of that type in rural areas. The first model of this type, system G1, totally collapsed under a relatively moderate earthquake due to wall separation. After this, all the stone-masonry models tested at ISMES were prior-strengthened. Stone masonry systems built and tested at LEE had the same quality of mortar as the ones built in Italy

Figure 2. Three ISMES buildings (brick masonry). The central building is strengthened by rb

Table I. Masonry and mortar strengths

Type of specimen	Strengths (Mpa)		Sizes (cm)	Number of specimens	
	Compression	Diagonal		Compression	Diagonal
Stone walls	0·27	0·065	$100 \times 150 \times 22{\cdot}5$	4	4
Brick walls	2·20	0·226	$100 \times 150 \times 22{\cdot}5$	4	4
Mortar cubes	0·80	—	$5 \times 5 \times 5$ cm	50	—

but were of better workmanship, as far as the connection of orthogonal walls and the jambs are concerned. Tests on their original unstrengthened configurations were carried out with shakings of lower maximum severity than the one producing the collapse of G1. Wooden slabs supported by wooden beams were always used. However, some models built at ISMES showed some improvement of the connection between slabs and walls in their original configuration. This was achieved by steel connectors on the beams and the slab. Figure 4 shows such devices, which will be referred to as sc. After being damaged in their original configurations (possibly slightly improved by sc devices) the models were repaired and strengthened by a number of different techniques briefly described below, due to space limitations. Details are given in References 1–3.

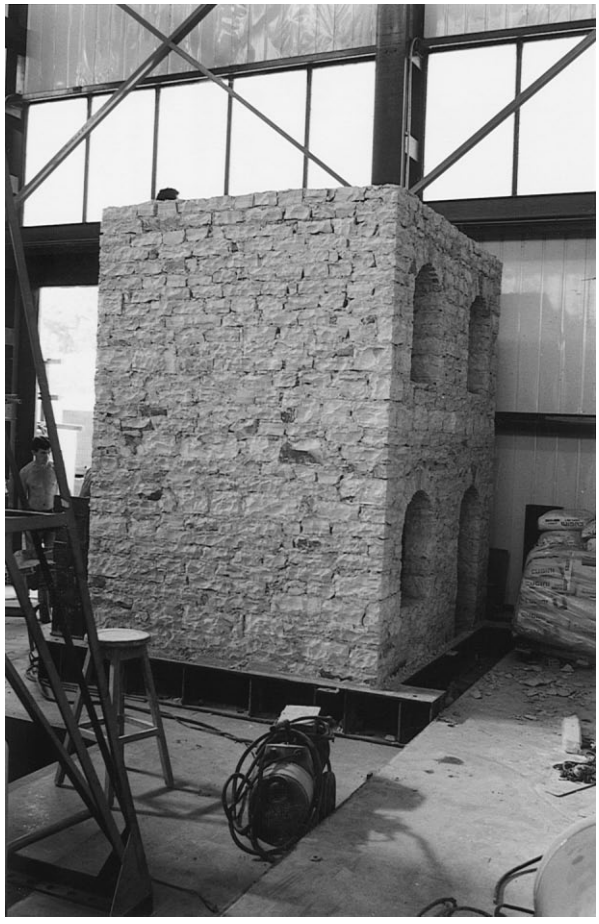

Figure 3. A building tested at LEE (stone masonry and arches)

2.3. *Strengthenings and repairs*

Major cracks were repaired by local sealing, using cement mixture (lsc), emaco (lse) or gypsum (lsg). The two last systems were used at LEE and the first one at ISMES. Several methods were employed to improve the connection between slabs and walls. Steel networks were nailed to the slabs, bent over the surrounding walls, connected to them and covered with a cement layer (sn*i*, where *i* denotes the storey level). Figure 5 shows an example of this intervention. In some cases (at ISMES) steel networks were placed at each storey level all around the building and covered with a shallow cement layer, thus originating a reinforced concrete band at those locations (rb). A building strengthened in this way is shown in Figure 2. In some instances horizontal tendons (ht) were applied at each storey level. To keep their action constant, a spring was placed between end bolts and the device used to transmit the action to the walls. These devices were either vertical steel beams placed at the corners of the building (vb) or horizontal steel beams spanning the whole length of the wall (hb), or wooden plates (wp) outside walls, at mid-height and the top, to achieve a better distribution on the wall of the confining action of the horizontal tendons. For Greek buildings, the arches over windows and doors were strengthened through the application of two light curved steel blades at both faces of the intrados. This intervention is labeled (a1) or (a2), where

Figure 4. Improvement of the connections of slabs to walls by steel anchors (sc)

Table II. Buildings tested at ISMES

Building	Mat.	Conf.	Repair/ strengthening	Input	No. of shocks
A1	Br	c1	sc	S	5
A2	Br	c1	lsc-rb-sn2	S	6
B1	Br	c1	—	L	5
B2	Br	c1	lsc-sn1,2	L	5
C1	Br	c1	—	L	4
C2	Br	c1	lsc-ht-sn1,2	L	5
D1	Br	c1	sc	S	5
D2	Br	c1	lsc-ht	S	7
E1	St	c2	sc-rb	S	5
F1	St	c2	sn1,2	S	4
G1	St	c3	—	S	4
H1	St	c3	sc-ht	S	3

the number denotes the storey level whose arches are treated thus. Figure 6 shows an ISMES building strengthened by ht, Figure 7 an LEE building strengthened by ht and wp and Figure 8 an LEE building in which arches at the first storey level have been strengthened (a1); the building is also strengthened by vb and ht.

Figure 5. Steel network and cement layer over the slabs (sn)

Table III. Buildings tested at LEE

Building	Mat.	Conf.	Repair/ strengthening	Input	No. of shocks
I1	Br	c2	—	S	4
I2	Br	c2	lse-vb-ht-a2	S	6
L1	Br	c2	—	S	5
L2	Br	c2	lsg-hb-ht	S	6
M1	Br	c2	—	S	6
M2	Br	c2	lsg-wp-ht-hb-a2	S	6
N1	St	c2	—	S	2
N2	St	c2	lsg-vb-ht	S	5
O1	St	c2	—	S	2
O2	St	c2	lsg-vb-ht-a1	S	6
P1	St	c2	—	S	3
P2	St	c2	lsg-wp-ht-a1-hb	S	5

Tables II and III show the configurations of all the buildings tested at ISMES and LEE respectively. Each building is represented by a letter (A, B, etc.) and a number (2 for repaired buildings and 1 for the original ones). Repaired buildings are thus denoted by codes A2, B2, etc., while buildings in their original configurations by codes A1, B1, etc. Note that the two tables also show the input used during the tests (S = short

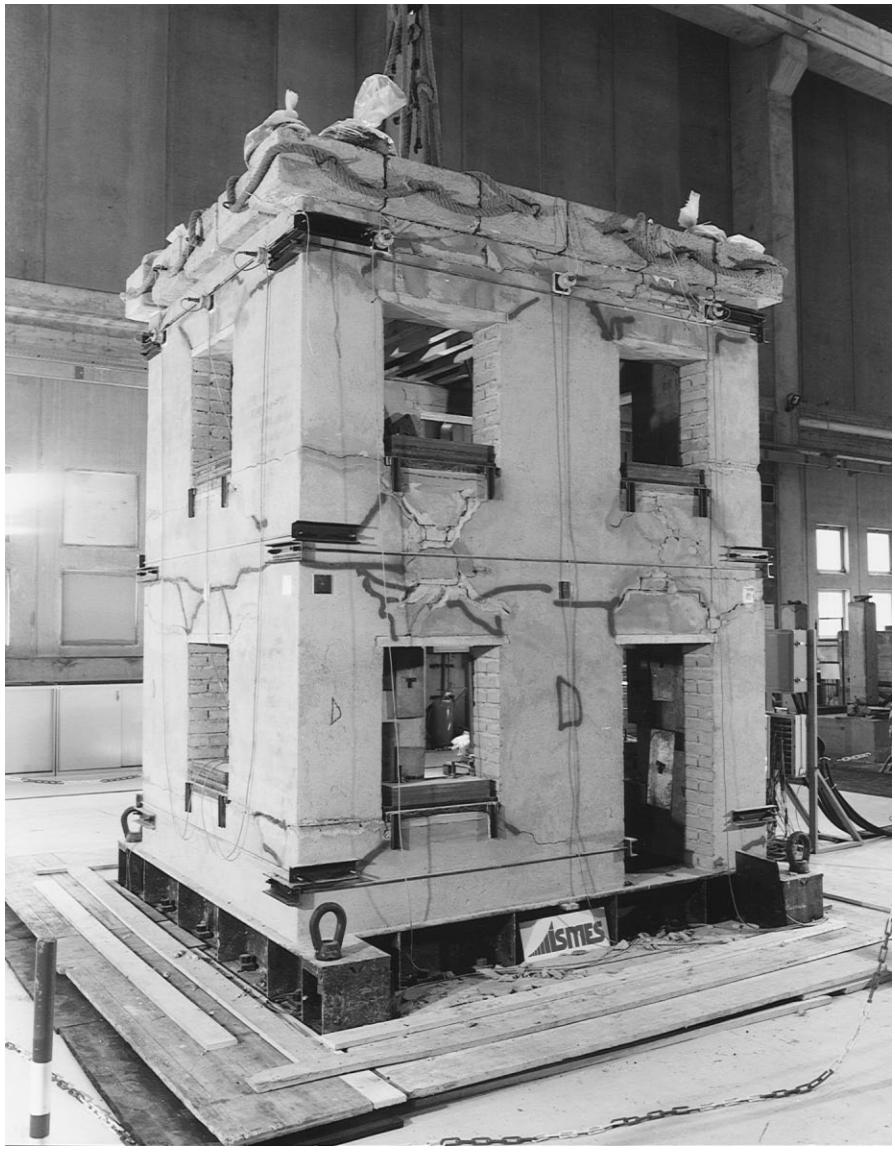

Figure 6. Building D2, strengthened by ht, before the ultimate shock

excitation set, L = long excitation set), which will be discussed in the next section, and the total number of shocks N. Repairs and strengthenings used are described by the codes presented above.

3. BASE INPUTS

Simultaneous base excitations, acting along two orthogonal horizontal directions and the vertical one, were applied to each building; the peak values of vertical accelerations being about 70 per cent of the peak values of the horizontal ones. Each building was subjected to a group of N of the above sets of inputs, the sets being obtained by scaling accelerations by a progressively increasing factor. The values of N for each building are

Figure 7. Building M2, strengthened by wp-ht-hb-a2, after the last shock

shown in Tables II and III. For the first set, the scale factor gives rise to base inputs with peak accelerations of the order of 5 per cent g, so that the building response is linear elastic. For subsequent sets of the same group, scaling factors are increased up to ultimate conditions for the building. Hence, all sets of base inputs of a given group are identical in frequency contents but different in acceleration values.

The use of peak accelerations to characterize input sets acting on a given building only gives a poor description of the severity of the earthquake and its damaging capacity. However, since input sets are obtained by scaling the same reference base excitations of a given factor, inspection of such values enables comparison of the severity of the shocks leading the various buildings to ultimate.

Two reference base input sets were used during the tests, both derived from the signals recorded at Calitri during the 23 November 1980 Irpinia earthquake. The first set accounts for the whole duration of the signals. As an example, Figure 9 shows the base acceleration in x-direction normalized to the peak value; signals acting in the orthogonal horizontal direction and along the vertical one are similar to it. Their basic features are the long duration (about 90 sec) and the sequence of two main shocks of similar peak acceleration. These excitations are labeled L in Table II. The second type of reference input consists in the first section of the long input, of about 40 sec duration.

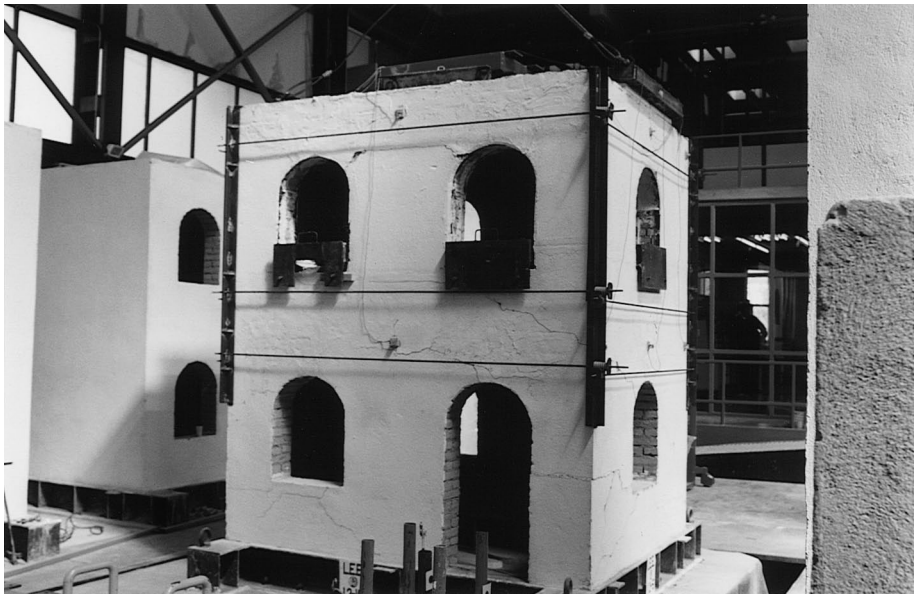

Figure 8. LEE building strengthened by vb-ht-a2, after a moderate shock

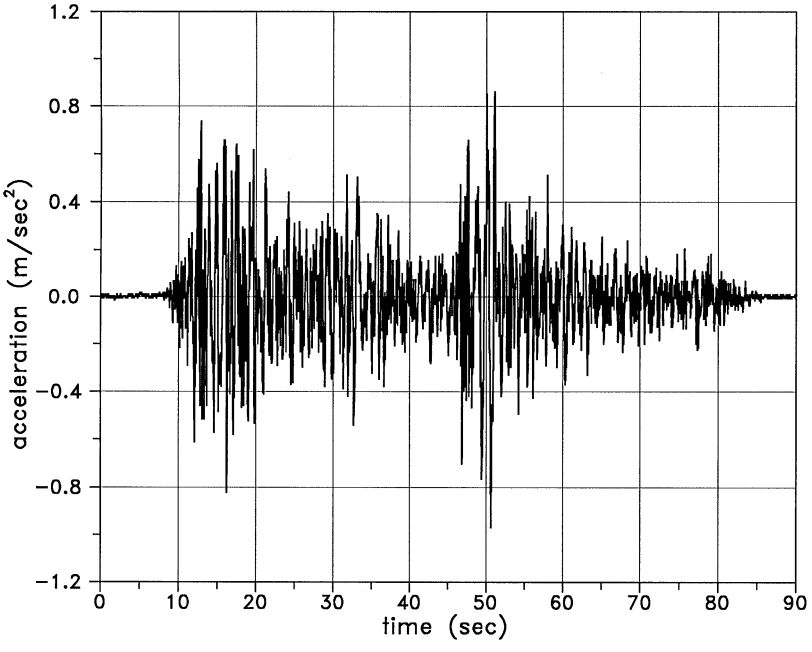

Figure 9. Base acceleration in the x-direction (long duration) normalized to peak value

These shorter excitations (label S in Tables II and III) have a frequency content similar to that of excitations L. Figure 10 shows the response spectra of the S and L base x-accelerations, normalized to their peak values. In both instances, major spectral amplifications occur for frequencies between 1 and 5 Hz, i.e. in the range of frequencies of the fundamental modes in x-direction of the tested buildings, in both their original

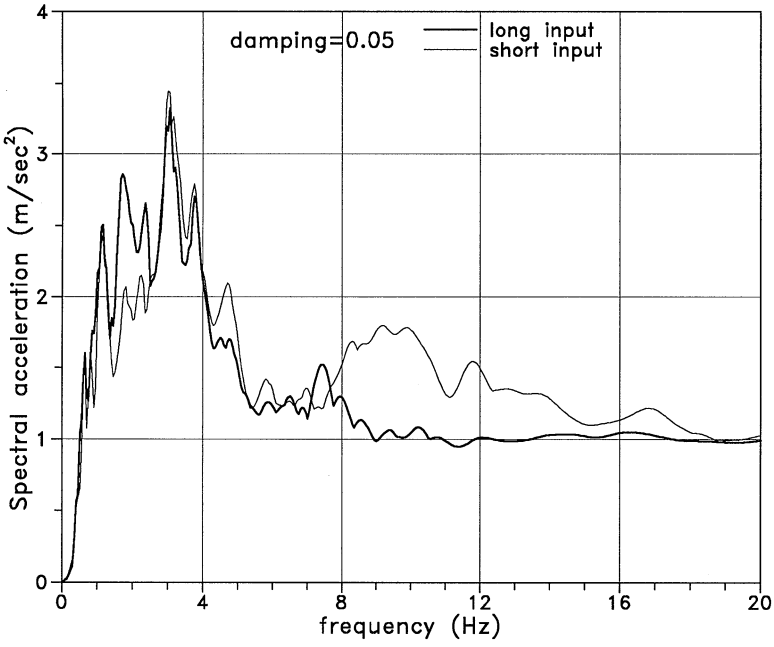

Figure 10. Acceleration response spectra (5 per cent damping) of L and S base inputs in the x-direction

and ultimate states (see Tables V and VI). Similar features hold for spectra of the excitations in the y-direction.

4. INTERPRETATION OF TEST RESULTS

This section describes the main steps in the interpretation of test results, giving comments and examples for each step. Results are referred to the real scale, as said, and reference is often made to ultimate conditions. These refer to the last shock of each testing sequence pertaining to a given building, during which it suffered heavy damage. In a few cases the last test was interrupted due to early collapse of the system and in one case total collapse took place. Due to the need of protecting testing equipment and allowing the transportation of models away from the shaking table to perform repairs and strengthenings, testing sequences were halted before the true ultimate conditions of the considered buildings were reached. Hence, the word 'ultimate' refers to the conditions of the structures during the last test. They may, however, be considered rather close to the true ones.

4.1. Damage pattern and amplifications

After each test of given sequence, cracks were accurately mapped. In all original systems spandrel beams were severely affected by cracks. This suggested the implementation of repairs aimed at strengthening these parts of the structure (such as rb). In some (but not all) instances diagonal cracks were observed in piers, mainly in those at the first level. Very frequently, piers were heavily damaged at their top and bottom bases (see Figure 11) by wide horizontal cracks that almost sheared them off from the remaining wall. Wall separation occurred only in ISMES stone masonry buildings, and in one case (G1) it produced the total collapse of the building. Figure 12 shows the main stages (shots A–F) of the failure.

Figure 11. Heavy damage at the bases of piers at the first storey

For each shock, amplification factors were computed at the two-storey levels, with reference to the response in the x-direction. These are the ratios of the maximum response acceleration recorded at a given location to the peak value of the base acceleration in the same direction. The responses at the two storeys are obtained by averaging the signals recorded at locations 1 and 3 (second level) and 11 and 13 (first level) of Figure 1. Locations 2 and 12 are not taken into account since they include the out-of-plane behaviour of y-walls. For undamaged buildings, amplifications are rather high, of the order predicted by elastic response spectra, thus showing a basically linear response. At the first level, the average value detected for Br buildings is 1·43 while for St systems it is 1·46. At the second level, initial amplifications are, respectively 2·41 (Br) and 2·23 (St). In all cases the coefficients of variation do not exceed 15 per cent, showing a substantial homogeneity of the buildings of each type. At ultimate, amplifications decrease with respect to the initial ones by about 27 per cent (both for St and Br systems) at the first level and by 35 per cent at the second level. After repair, initial amplifications for brick-masonry buildings are 90 and 75 per cent of the original (undamaged) values, at the first and second storey, respectively, thus showing the efficiency in recovering the original properties of the technical interventions carried out. During the last shocks, amplifications of repaired systems show a lower decrease with respect to the initial ones than that observed for the original undamaged systems (15 and 25 per cent at the first and second storey, respectively). This may be a consequence of a more compact behaviour up to ultimate, achieved by the considered strengthenings.

4.2. Connection of slabs to walls

The efficiency of slabs in connecting x-walls was analysed by comparing the response accelerations recorded at points 5–8 and 15–18 of Figure 1. These points define the mid-span of walls along x-direction

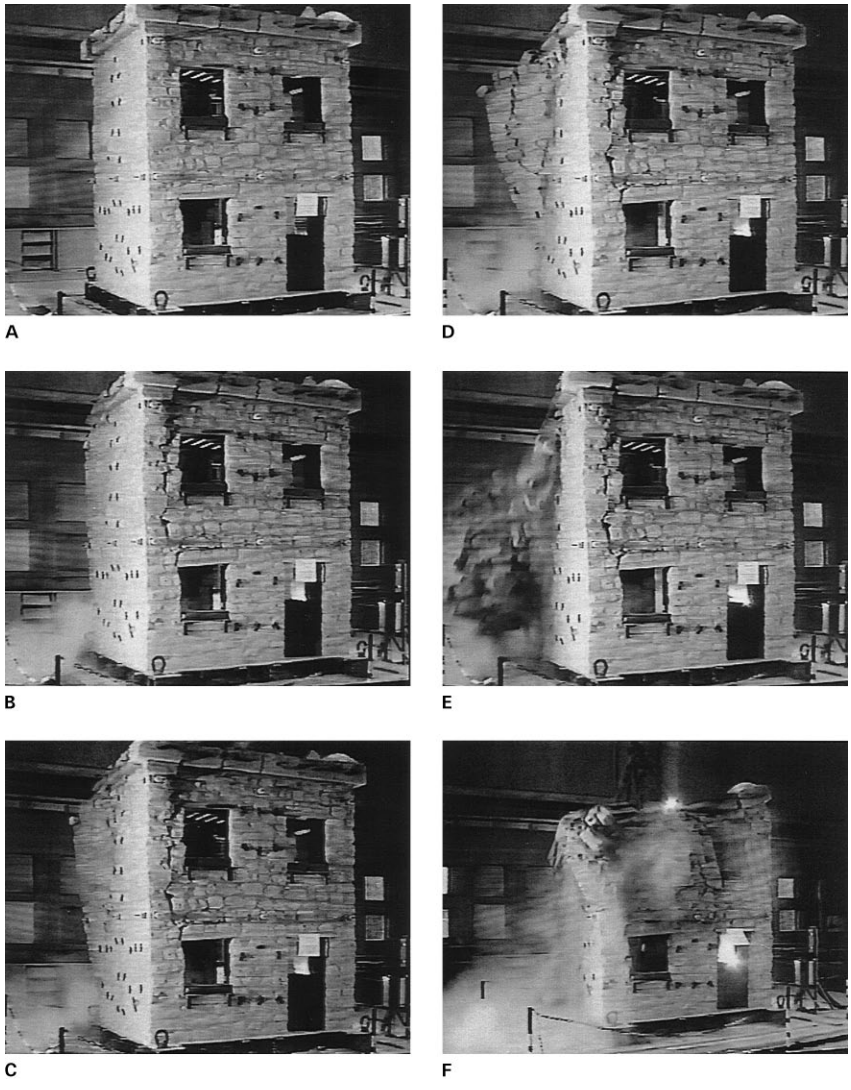

Figure 12. The collapse of building G1

at the two-storey levels. Note that slabs are supported by these walls. The maximum shift (ranging from 6 up to 50 per cent for the buildings taken into account) is a measure of the independence of the out-of-plane behaviour of the two opposite walls during a given excitation. Then, the phase angle of the cross-correlation functions, evaluated by considering the signals recorded at the said pairs of points, is computed. If the two responses (at 5 and 8 or at 15 and 18) are in phase, the two opposite walls move in the same direction during the earthquake, which proves a good quality of the considered connections. As an example, Figure 13 shows the phase of the cross-correlation function computed at locations 5–8 during the last shock for the system D1. As can be seen, the two walls behave independently (phase angle $\cong 180^\circ$) for frequencies higher than 9 Hz. Note that for the repaired system D2 (lsc-ht) no independent behaviour is observed (phase function not shown here).

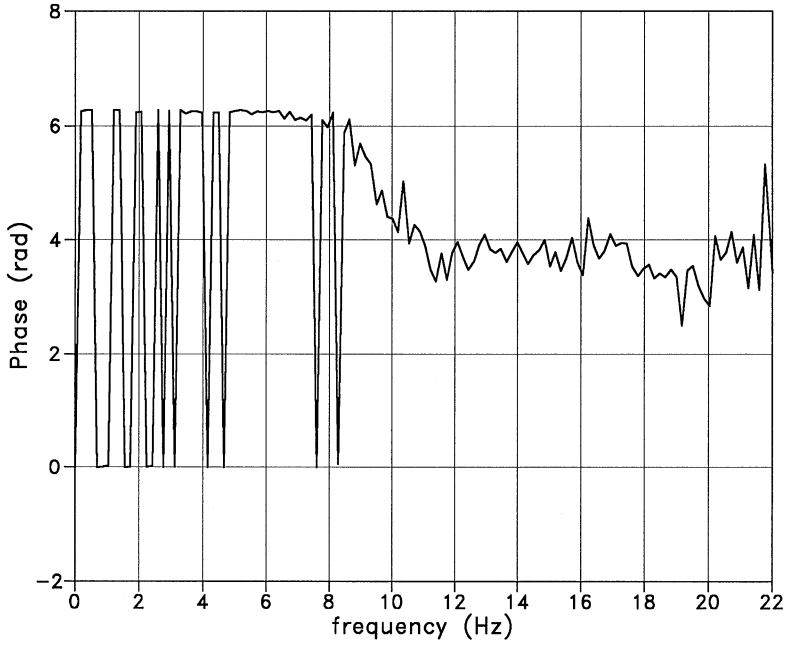

Figure 13. Phase of the cross-correlation function between points 5–8 (second level)

4.3. Identification of dynamic properties

For all the buildings tested at ISMES and some of those tested at LEE an identification procedure was used to estimate the modal properties of the systems during the N input sets specified in Tables II and III. Identifications were made by a procedure which takes into account the effect of two simultaneous orthogonal horizontal base inputs on responses.[4] Four quantities had to be identified for each mode at the considered location. By calling r the mode number and i and j the two orthogonal horizontal directions of the base inputs, they are (a) the modal frequency f^r and damping ζ^r; (b) the effective participation factor β_{ii}^r describing the contribution to the response in the direction i of the rth mode (at the considered location) due to the base input acting in the same direction i; (c) the effective participation factor β_{ij}^r describing the contribution to the same response of the base input acting transversally to it, i.e. along the direction j. In the case of a sway mode and of an ideal structurally symmetric system $\beta_{ij}^r = \beta_{ji}^r = 0$, when symmetry fails to hold, the effective participation factors with indices $i \neq j$ are, in general, non-zero. This condition may also arise as a consequence of the loss of symmetry due to the differential state of damage suffered by the resisting elements. On the other hand, systems originally non-symmetric, with initial values $\beta_{ij}^r \neq 0$ $(i \neq j)$, may show a decrease of the absolute values of such 'indirect' participation factors at the increase of the severity of the shaking and of the consequent increase of the damage suffered by the system. This feature may appear if the building loses its box-type behaviour, particularly when the connections between orthogonal walls, though not showing separation, do not allow the transmission of moments acting in horizontal planes, so that the response in one direction cannot be influenced by the excitation acting along the orthogonal direction. This turned out to be the case for several systems strengthened by the use of horizontal tendons. Hence the evolution of β_{ij}^r $(i \neq j)$ during a given group of earthquakes may be considered as a description of the progressive state of damage and of its influence on the response mechanism. Moreover, the values of these coefficients after repairing and strengthening the damaged structure supply information about the efficiency of repairs, as far as the overall structural organization is concerned.

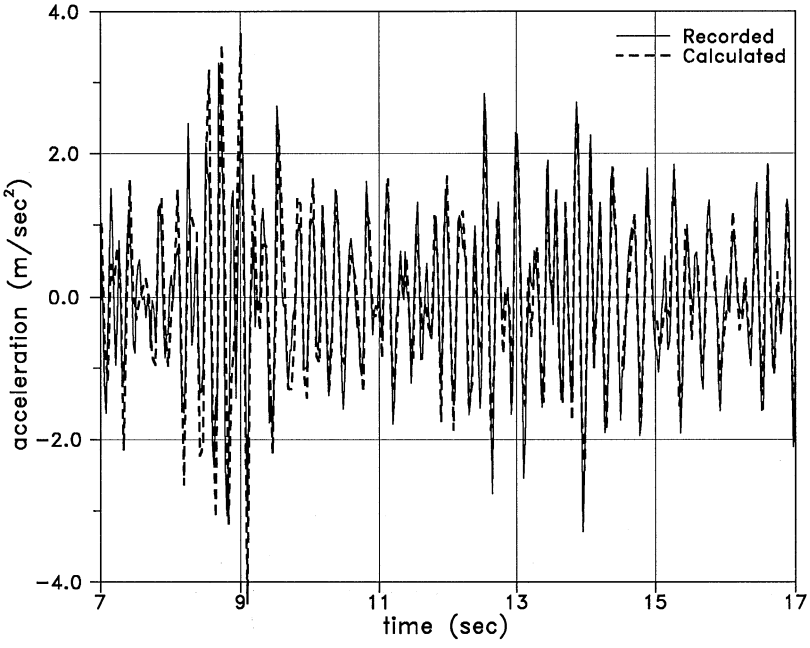

Figure 14. Calculated and recorded relative acceleration at point 2, building D1, time: 7–17 sec

To detect torsional modes, for all the base inputs considered, the cross-correlation function between responses at laterally spaced locations (such as 1–3, 14–16, 11–13) was calculated and its phase analysed. Torsional modes are always detected during the very first excitations for all buildings. However, at the increase of damage suffered by the systems they tend to become less significant and in some instances disappear, as a consequence of the loss of the 'box-type' behaviour of the buildings.

Identifications were carried out to detect the first 5 modes, with reference to the responses recorded at point 2 (in the x-direction) and at point 14 (in the y-direction). Modal parameters thus identified, although referred to an equivalent linear system, allow us to describe the evolution of the structure from its virgin state (first shock) up to its ultimate state (last shock) and to assess the efficiency of strengthenings by comparing the relevant modal quantities. The quality of the identification was checked by computing responses at points 2 and 14 through modal superposition. The computation involved the following steps: (a) first, the transfer functions in the frequency domain of the relative response accelerations at the selected locations were built up by using the whole set of the identified modal parameters; (b) then, the FFT of the pertinent base inputs were calculated; (c) the product of the above functions gave finally the response accelerations in the frequency domain: their Inverse Fourier Transform provided responses in the time domain. Calculated responses were compared to the recorded ones. In general a good (sometimes very good) agreement was found to hold. As an example, Figure 14 shows (in the time window 7–17 sec, during which the main part of the response occurs) the recorded and the calculated relative accelerations in the x-direction at location 2 for the building D1 during an intermediate shock (PGA about 23 per cent g), acting on a structure damaged by previous excitations. In this case, identified frequencies and damping showed a decrease of about 24 per cent (modal frequencies) and an increase of about 50 per cent (damping) with respect to the original values. In Section 5 some modal parameters, pertaining to the first and last shocks of ISMES buildings, are presented and discussed. The complete results of the identifications carried out (10 modes for each shock and each building) are reported and commented on extensively in Reference 2.

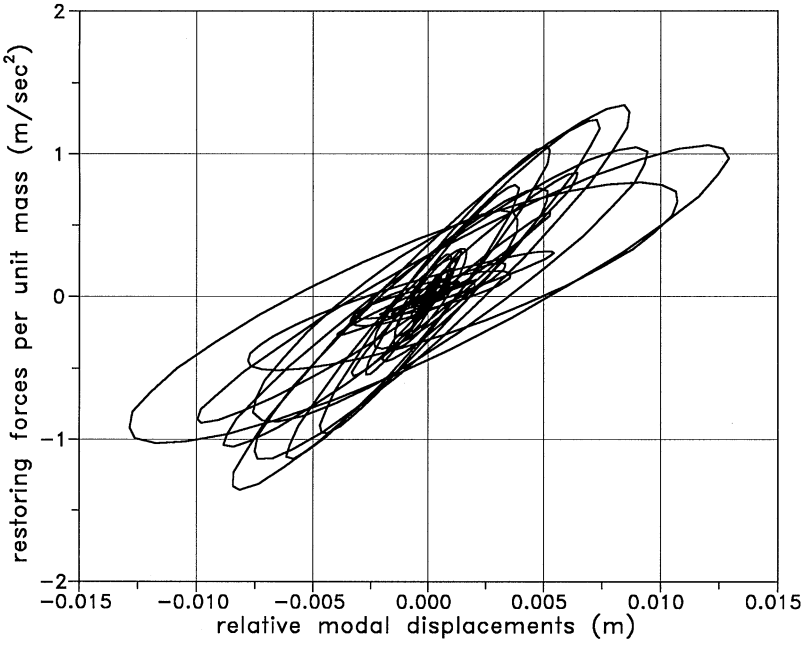

Figure 15. Restoring forces per unit mass of the first x-mode, system E1, ultimate shock

4.4. Effective stiffness of the fundamental mode

During non-linear responses, modal parameters determined by identification refer to a linear system, equivalent to the actual non-linear one for the considered excitation. In order to point out the variation of modal quantities during the response, restoring forces and the effective stiffness (see Reference 5) associated with the fundamental mode in x-direction (location 2 of Figure 1) were analysed for all the buildings tested at ISMES and some of those tested at LEE.

Although modes do not strictly exist for a non-linear system, it is possible to separate the response into 'mode-like' contributions, dominated by a narrow frequency content. In fact, it was shown by several researchers—starting from the pioneering work by Rosemberg[6] up to the latest works by Iwan and Peng[7] that a sort of modal decomposition may be carried out in the non-linear phase too and that modal coupling may be eliminated by means of appropriate mathematical transformations or through appropriate filtering of the response. In these analyses, response signals were narrow-band filtered around the identified frequencies of the first mode acting primarily in the x-direction. Then, the evolutions, during the considered excitation, both of restoring forces and of the effective stiffness against the modal relative displacements, were worked out. As an example, consider Figure 15 showing the r.f. cycles pertaining to the fundamental mode of the system E1 during the last shock of the sequence. The change of width of loops and the decrease of the slope of their major axis is apparent. The first item correlates to the variation of the dissipation capacity during the shock (being here the frequency content of the signals limited to a very narrow band), while the second item describes the evolution of the effective stiffness (defined as the ratio of the r.f. at the maximum displacement of a given cycle to such displacement) during the excitation. This fact may also be seen by considering the variation of the effective stiffness with respect to maximum cycle displacements and to time. To this latter aim, a particular time scale is used, which corresponds to displacements exceeding a given value, in order to avoid numerical malfunctions due to very low values of displacements occurring in very small cycles (note that in k_{eff} these displacements divide the restoring forces). This time scale, which may be

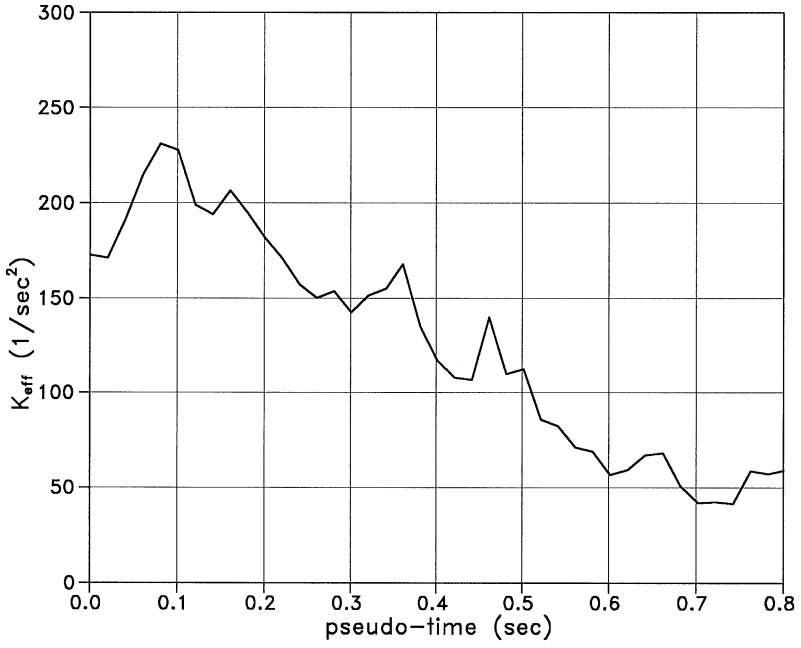

Figure 16. Variation of k_{eff} of the first x-mode during the ultimate shock, system E1

roughly considered to be proportional to the real time scale during the meaningful portion of the signal, is called pseudo-time. As an example, Figure 16 shows k_{eff} with respect to pseudo-time for the system E1 during the last shock. As can be seen, a progressive deterioration of the stiffness occurs during the response. At its end, k_{eff} is reduced to about 30 per cent of its value at the beginning of the earthquake. Note that the physical dimensions of k_{eff} are those of the square of a circular frequency ($1/\text{sec}^2$). For linear systems k_{eff} corresponds to the actual frequency of the considered mode. Here, the identified frequency of the first x-mode corresponds to the average value of k_{eff} during the whole response. In other instances, this is not the case and identified frequencies during strong shocks correspond to the values of k_{eff} during a section of the excitation. The analysis of the variation of k_{eff} helps us to understand the changes in the response mechanism during a single strong excitation or a whole set of earthquakes.

4.5. Lateral forces–displacements relationships and structural reduction factor q

Lateral forces acting on the buildings during each excitation set were computed with reference to x-direction only. They were determined by multiplying the response absolute accelerations at selected locations of y-walls by the pertinent mass. Forces are expressed as ratios to the total weight of the real building, thus expressing the base shear coefficients C during the considered base input. After integrating twice the relative acceleration in x-direction at point 2, the displacement time history is obtained. This is correlated to lateral forces, constructing the global loading–unloading cycles of the system. By considering these cycles for all the excitation sets of a given building, information about the variation of dissipation characteristics and about the change of behaviour from linear to non-linear may be easily recovered. On the basis of the cycles thus obtained, the envelope load–displacement curve can be determined, by considering all the earthquakes to which the given system was subjected. As an example, Figure 17 shows the (C-displacements) values referring to the whole set of events acting on the system B2. The envelope curve of such C values allows us to estimate the maximum base shear coefficient C_{u} and the one at the significant yield C_{y}.

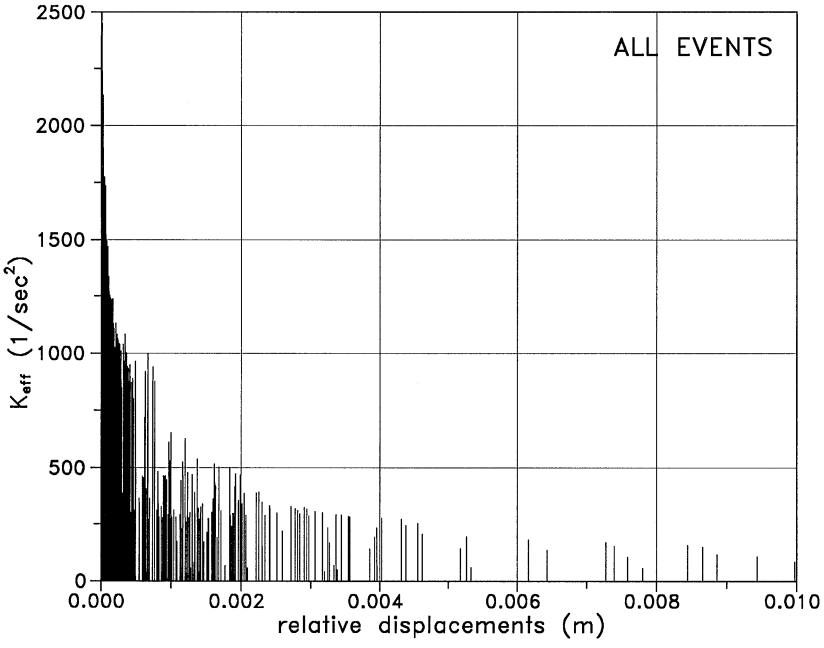

Figure 17. Lateral forces vs. displacements of the second storey for building B2, all events

Table IV. Lateral force coefficients and reduction factors for ISMES tests

	A1	A2	B1	B2	C1	C2	D1	D2	E1	F1	G1	H1
P_y	3	4	4	3	2	3	3	3	3	—	3	3
C_y	0·19	0·205	0·22	0·20	0·21	0·15	0·155	0·20	0·11	—	0·09	0·09
C_e	0·30	0·36	0·33	0·43	0·31	0·41	0·30	0·36	0·24	—	—	0·16
C_u	0·22	0·30	0·30	0·31	0·25	0·30	0·26	0·29	0·19	0·11	—	0·12
q	1·6	1·8	1·5	2·15	1·5	2·7	1·8	1·8	2·2	—	—	1·8

The latter corresponds to the maximum lateral force occurring during the excitation P_y that causes the first significant change in the response. This shock is selected from the whole set of excitations by considering the evolution of the damage pattern and that of the identified dynamic properties and the effective stiffness. Although the behaviour of the structure from its undamaged configuration up to the event P_y producing the force C_y cannot be considered as strictly linear, it is however linearizable, as suggested by ATC-3. By using the dynamic properties identified during P_y, the response under the event causing ultimate conditions can be calculated by modal superposition. It provides the maximum lateral force C_e that would act on the structure, under the action of the ultimate earthquake, if the system behaved linearly. After estimating C_e and C_y, the structural reduction factor q is evaluated, according to the definition given by ATC-3, as the ratio of C_e to C_y. Table IV reports (for ISMES tests) the values of C_u, C_e, C_y, q thus determined and the code of the excitation set during which the significant yield occurred.

For the system G1 the above computations could not be carried out completely due to the total collapse of the structure after the excitation producing the significant yield. For the system F1, table malfunctions caused severe damage during the first test, hence linear (or linearizable) properties could not be estimated.

5. COMPARATIVE REMARKS FOR ISMES TESTS

Table V summarizes the main results obtained for the systems A–H. Column 2 (mat) describes the material type of the building; column 3 describes the type of repair or strengthening carried out; columns 4, 5, 6 and 7 ($f_{xi}, f_{xf}, f_{yi}, f_{yf}$) show the frequencies of the first two modes (primarily in x and y direction) determined during the first and the final shocks of the base input set pertaining to the considered building; columns 8, 9, 10 and 11 report damping values ($\zeta_{xi}, \zeta_{xf}, \zeta_{yi}, \zeta_{yf}$ in per cent to critical) of the same modes and the said events; columns 12 and 13 (C_y and C_u) show the lateral force coefficients at the significant yield and at ultimate, respectively, and column 14 (q) the estimated structural reduction factor; columns 15 and 16 show the values of the horizontal peak accelerations a_{Mx}, a_{My} of the ultimate shock. Finally, column 17 shows (in per cent to the maximum recorded response) the maximum shift between the response accelerations recorded at the mid-span of x-walls during the last excitation, providing a measure of the quality of the connections between x-walls and slabs.

Note that, due to the total collapse of the building G1, final frequencies of Table V refer to values identified during the shock immediately before the one producing the total collapse, while the peak acceleration values reported for G1 refer to the shock causing collapse. Also note that C_y and q are missing for the system F1, due to the fact that malfunctioning of the table caused heavy damage to the structure, which produced a non-linear response during the first shock of the testing sequence. C_y, C_u, q and the shift value for G1 are missing due to the collapse. Inspection of Table V and the analysis of test results suggest the following comments.

5.1. *Frequencies and damping*

(1) For original brick-masonry systems, (A1, B1, C1, D1), frequencies of the first x-mode range from 4·6 to 6 Hz while those of the first y-mode range from 5·37 to 6·76 Hz. In both cases, the lowest frequencies are about 80 per cent of the highest, showing a substantial homogeneity of construction. Moreover, in all cases f_x and f_y are rather similar, showing structural symmetry holding initially for the said systems. The highest shift between f_x and f_y is recorded for system C1, and is of the order of 20 per cent.

(2) Such frequencies show a considerable reduction during ultimate shocks, being up to 30 per cent of the original values. This proves the important state of damage suffered by the systems. With the exception of the building A1, final frequencies of the said modes turn out to be less close to each other than they were in the virgin state of the systems, thus showing the different damage suffered by walls in x- and y-directions, determining structural dissymmetry.

(3) The only stone-masonry system tested in its original configuration, without any prior strengthening, was G1. Its initial frequencies are about 50 per cent of the average initial frequencies identified for brick-masonry buildings. This points out a (deliberate) poorer quality of construction of the stone-masonry system compared with that of brick-masonry units. It is also confirmed by the rather low initial frequencies of prior-strengthened buildings F1 and H1. On the other hand, initial frequencies of E1 (for which a r.c. band is applied at each storey level) are of the same order as the average ones determined for brick masonry.

(4) Initial damping of the fundamental modes varies from 6% to 10% to critical for undamaged brick masonry, while for the initially undamaged stone-masonry system (G1) it is about 10% to critical. These values are consistent with what is expected for these types of structures.

5.2. *Effects of repairs on frequencies and damping*

(1) Repairs and strengthenings carried out on damaged buildings, even the very simple ones, such as D2, practically recovered original frequencies and, in some instances, increased them. For stone-masonry systems subjected to prior strengthening (E1, F1, H1), initial frequencies are equal to (F1) or higher (E1, H1) than the values obtained for the building (G1) tested without any strengthening device.

(2) Original dampings were recovered (and in some instances lowered) only when local sealing of major cracks was used in conjunction with interventions able to recover a 'compact' behaviour of the systems

Table V. Main results of ISMES tests

1	2	3	4	5	6	7	8	9	10	11	12	13	14	15	16	17
Building	mat	rep./str	f_{xi} (Hz)	f_{xf} (Hz)	f_{yi} (Hz)	f_{yf} (Hz)	ζ_{xi} (%)	ζ_{xf} (%)	ζ_{yi} (%)	ζ_{yf} (%)	C_y	C_u	q	a_{Mx} (m/s^2)	a_{My} (m/s^2)	max shift
A1	Br	sc	4·6	1·91	5·37	2·12	6·0	19·0	5·8	31·0	0·19	0·22	1·6	3·20	2·70	39·0
A2	Br	lsc-rb-sn2	6·0	2·55	6·03	2·06	16·0	35·0	8·5	26·0	0·21	0·30	1·8	3·51	4·40	7·0
B1	Br	—	6·05	3·50	6·28	4·70	11·5	31·8	8·4	18·8	0·22	0·30	1·5	2·98	3·42	30·0
B2	Br	lsc-sn1,2	5·80	1·98	6·10	2·65	14·0	21·0	9·0	37·0	0·20	0·31	2·15	4·43	3·72	16·0
C1	Br	—	5·06	1·44	6·22	2·25	10·8	28·0	10·8	41·0	0·21	0·25	1·5	2·75	2·90	48·0
C2	Br	lsc-ht-sn1,2	5·41	2·49	5·60	2·79	7·0	15·0	10·3	32·0	0·15	0·30	2·7	4·49	4·45	14·0
D1	Br	sc	6·06	3·44	6·76	4·41	5·8	10·0	4·5	16·0	0·15	0·26	1·8	2·89	3·10	15·0
D2	Br	lsc-ht	5·44	3·52	6·04	3·90	5·8	12·5	6·6	18·8	0·20	0·29	1·8	2·77	3·18	6·0
E1	St	sc-rb	5·25	1·88	5·83	2·20	18·2	42·0	18·6	44·0	0·11	0·19	2·2	2·40	2·33	25·0
F1	St	sn1,2	2·40	1·88	3·04	1·48	13·2	24·0	15·6	35·0	—	0·11	—	1·51	1·65	15·0
G1	St	—	2·37	1·93	3·29	2·50	7·00	9·0	10·3	13·0	0·09	—	—	1·50 coll.	1·89 coll.	—
H1	St	sc-ht	3·88	1·57	4·31	1·93	10·0	20·0	15·0	18·0	0·09	0·12	1·8	1·49	1·58	18·0

Note: sc = steel connections of slabs to x-walls
rb = bands at each level (steel network + cement layer)
sn1,2 = steel network + cement layer over slabs (wrapped over the walls) at level 1, 2
lsc = local cement sealing of major cracks
ht = horizontal tendons

(horizontal tendons and /or r.c. layer on both slabs), as happens for B2, C2 and D2. The use of r.c. bands at each storey level (A2) proved unable to recover original damping properties. Furthermore, in the case of stone masonry (E1 strengthened by r.c. bands) initial damping is higher than that determined for G1, F1 and H1.

5.3. *Base shear coefficients and q factors*

(1) Ultimate base shear coefficients C_u estimated for brick masonry, range from 0·22 to 0·3. After repairs and strengthenings a common value (about 0·3) is achieved in all cases, even when a low cost intervention takes place (D2). For stone masonry, C_u values are lower, ranging from 0·11 to 0·19, consistent with the poor quality of construction. Base shear coefficients at significant yield C_y range from 0·15 to 0·21 for brick-masonry and are about 0.09 for stone-masonry systems. For repaired systems C_y values are rather erratic with respect to the original values; ranging from 0·15 (C2, original value 0·21) to 0·20 (D2, original value 0·15). This may be due to the non-predictable behaviour of local sealings that, in some cases, fail rather early and in others withstand larger excitations.

(2) Structural reduction factors q estimated for brick-masonry buildings in their original configurations are rather similar, ranging from 1·5 to 1·8. They are of the order of magnitude expected for unreinforced brick-masonry systems. Repairs and strengthenings recovered (D2) or improved (A2, B2, *C*2) the original ductile behaviour, as expressed by the q-factor. For the latter buildings the increase of q ranges from 15 to 60 per cent with respect to the original values. As a consequence of this increase, the 'intensities' of the ultimate shocks (roughly described, as said, by the peak base accelerations) for such systems were 40–60 per cent higher than the corresponding ones of the original systems. For stone-masonry buildings the reduction factor q is of the order of $q = 2$, slightly higher than the average value estimated for brick-masonry. Note, however, that both E1 and H1 were subjected to prior strengthening.

5.4. *Efficiency of repairs*

(1) In the original systems, a tendency to wall separation was sometimes observed (B1, C1, G1). However, the use of horizontal tendons or of r.c. bands or of r.c. layers wrapped over the walls, proved able to eliminate this failure mechanism. Repairs were not able to recover the capacity of transferring moments, acting in horizontal planes, between walls. This feature is pointed out by the weak importance of torsional modes in repaired systems and by the low values of the effective participation factors β_{xy}, β_{yx} accounting for the effect of the excitation acting transversally to the response. The values of the above participation factors and the properties of torsional modes are not given here due to space limitations.

(2) The efficiency of steel links of slabs to walls is questionable and highly dependent on the quality of construction. As an example, they prove efficient in the system D1 but inefficient in building A1. On the other hand, horizontal tendons, r.c. layers on slabs and r.c. bands significantly reduced the independent behaviour of walls and turn out to be always very effective.

(3) As said, local sealings of major cracks provide a satisfactory, though not complete, recovery of original damping properties. However, cracks in repaired structures tend to appear at the same locations as the original ones, as a consequence of the failure of sealings. When this happens the stiffness of the system shows a sudden decrease, as is apparent from the analysis of the evolution of k_{eff} during the shock.

6. MAIN RESULTS OF LEE TESTS

Table VI summarizes the outcomes of the tests on the systems I–P carried out at LEE. Since the full identification of structural properties from recorded signals is still in progress, the presentation will be limited to the main results. The meaning of items appearing in columns 1–7 is the same as for Table V. It should be

Table VI. Main results of LEE tests

1	2	3	4	5	6	7	8	9	10	11	12	13
Building	mat	rep./str	f_{xi} (Hz)	f_{xf} (Hz)	f_{yi} (Hz)	f_{yf} (Hz)	a_{Mx} (m/s^2)	a_{My} (m/s^2)	Rand	ρ_x	ρ_y	Damage
I1	Br	—	3·73	1·90	5·89	4·57	1·83	1·46	—	1·32	1·32	Extended damage mainly at spandrel beams at the second storey
I2	Br	lse-vb-ht-a2	4·67	3·45	4·57	2·84	2·73	4·12	R2, B1	0·59	0·51	Cracks in all piers, spandrel beams and *y*-walls
L1	Br	—	4·76	2·74	5·13	4·00	1·86	1·63	—	1·58	1·17	Same as I1
L2	Br	lsg-hb-ht	5·31	1·65	5·31	2·22	3·61	3·27	R6, B3	1·22	1·10	Almost collapse of the spandrel beams at the second storey. The horizontal steel beams almost 'cut' the walls
M1	Br	—	4·67	1·90	5·61	2·84	1·87	1·54	—	2·16	3·08	Same as I1
M2	Br	lsg-wp-ht-hb-a2	5·10	2·87	5·10	2·41	3·69	3·01	R3, B2	0·73	1·03	Heavy damage at the first storey (nearly collapsed) and at piers of *y*-walls
N1	St	—	4·52	2·38	4·67	3·94	1·58	1·06	—	1·36	1·09	Same as I1
N2	St	lsg-vb-ht	4·67	2·84	4·67	4·03	3·12	2·41	R5, S3	0·71	0·36	Failure of piers of *y*-walls. Collapse of the first floor slab
O1	St	—	3·81	3·45	5·37	4·64	1·13	0·84	—	0·82	1·60	Same as I1
O2	St	lsg-vb-ht-a1	4·94	1·90	5·19	4·03	4·12	4·12	R1, S1	0·95	0·40	Partial collapse of the second storey
P1	St	—	4·18	2·74	4·64	3·94	—	1·22	—	1·16	1·37	Same as I1
P2	St	lsg-wp-ht-a1	4·43	1·46	4·76	1·98	3·45	2·55	R4, S2	1·87	1·63	Extended damage at the first storey. Buckling of steel plates at the arches of the first storey. Failure of piers of *y*-walls

Note: hb = horizontal tie beams
ht = horizontal tendons
lse/g = local sealing of major cracks with emaco or gypsum
a1/2 = curved steel blades at the intrados of arches (first or second level)
wp = wooden plates at the spandrel beams
vb = vertical steel beams at the corners

noted that the value of the peak acceleration in x direction for the system P1 is missing, due to instrumental malfunction. Columns 8 and 9 report the values of the peak accelerations in x and y directions of the last shocks acting on the considered system. Column 10 describes the hierarchy of the strengthenings put into action. Such description is based on the ratios of the final PGA acting on the repaired system to the final PGA acting on the original building, which was about 15% of gravity acceleration for all the tested systems. The higher the ratio the better the effect of the considered strenghthenings. The letter R refers to the whole set of the considered buildings. Letters B and S refer to the classification of the effects for brick-masonry and stone-masonry buildings, respectively. As can be seen, the best effect of retrofitting is achieved for the system O2 (brick, R1) and the worst for the system L2 (brick, R6). For stone-masonry structures the best and the worst effects were detected, respectively, for buildings O2 (S1) and N2 (S3), while for brick masonry ones they were achieved, respectively, for systems I2 (B1) and N (B3).

Columns 11 and 12 (ρ_x and ρ_y) provide measures of the average velocities at which initial frequencies of the first x and y modes decrease at the increase of the severity of shakings of the relevant excitation sets. Indices ρ_x and ρ_y are the ratios $\Delta f/\Delta a$, Δf being the variation of the frequencies of the two said modes determined between the first and the last shock for a given building, and Δa being the variation of the peak base accelerations recorded for the two said shocks (in x- and y-directions).

In the results appearing in columns 10–12 the severity of shakings is described by their peak acceleration: as to this description and its intrinsic limitations the comments of Section 3 hold. Finally, column 13 contains a very synthetic description of the damage suffered by each structure.

Inspection of Table VI and the analysis of test results suggest the following comments.

6.1. *Variation of frequencies of the fundamental mode*

(1) Both for brick-masonry systems in their original configurations (I1, L1, M1) and for stone-masonry ones (N1, O1, P1), the lowest initial frequencies of the two fundamental modes are up to about 80 per cent of the highest ones. This feature is similar to what was observed for ISMES buildings and shows a substantial homogeneity of construction.

(2) These frequencies reduce significantly during the last shocks, being up to 40 per cent of the initial value (system M1). The reduction is more important for brick-masonry systems.

(3) With the exceptions of buildings I1 and O1, the initial frequencies of the two fundamental modes in x- and y-directions are rather close to each other. For the two said buildings, frequencies of the first x mode are lower than those of the first y mode, the former being up to 65 per cent of the latter.

(4) These features tend to disappear after repairs: for all the systems a substantial similarity of such frequencies is observed. This points out the efficiency of retrofitting in increasing stiffnesses in both principal plan directions. Moreover, repairs recovered original stiffness properties and, in almost all instances, increased them, as is shown by the values of initial frequencies of repaired systems.

(5) As shown by the values of ρ_x and ρ_y, the decay of the initial fundamental frequencies during the whole set of base inputs pertaining to a given structure, is quicker for the original systems than for the corresponding strengthened ones. This feature occurs for both stone masonry and brick masonry. It denotes the efficiency of retrofitting in giving the buildings a more homogenous behaviour up to ultimate than they had originally.

6.2. *Efficiency of repairs and strengthenings*

(1) No wall separation was observed in either original or repaired systems. This proves the good quality of construction and the efficiency of horizontal ties, constantly employed in all retrofittings.

(2) Severities of shakings (roughly described by their peak values, as said) leading strengthened structures to ultimate are always higher than those pertaining to the original (unstrengthened) systems. The increase of ultimate intensities (roughly described by peak values of base inputs, as said) depends only

on the type of strengthening and not on the material type of the original buildings. The detected global ranks (column 10) were in fact R1, R4 and R5 for stone masonry and R2, R3 and R6 for brick masonry.

(3) The best effects were achieved by using horizontal ties, vertical steel beams and curved steel blades placed at the intrados of the arches in the first or the second storey (strengthenings ht-vb-a1/2 applied to systems I2, M2 and O2).

(4) The worst performance was recorded for the system L2, for which the distribution on the walls of the actions due to horizontal ties was accomplished by horizontal steel beams. The damage pattern showed a tendency of the walls to be 'cut' by the horizontal beams. This fact points out the importance of an appropriate distribution of forces induced by the strengthenings. When this is made (e.g. by means of vb or wp) the behaviour of the repaired systems is fairly satisfactory.

7. CONCLUSIONS

The main achievements provided by the interpretation of the experimental results are as follows:

1. Significant increases of the lateral resistance, with respect to the original one, may be obtained by rather simple techniques, such as by the local sealing of cracks and the application of horizontal tendons. It is noteworthy that these improvements hold both for brick and for masonry systems, as shown by LEE tests.
2. The original quality of construction plays an important role in the benefits that may be achieved by strengthenings, in terms of ultimate lateral force coefficient and of ultimate base excitation. After retrofitting, originally well-built structures, even when severely damaged, reach ultimate conditions for excitations having peak accelerations of the order of 35–40 per cent of the gravity acceleration, thus proving able to withstand very severe earthquakes expected in Mediterranean areas.
3. Horizontal ties are very efficient in preventing collapse due to the separation of walls. Such devices were accomplished by steel ties, steel beams and r.c. bands. It was found that the best effects are achieved by an appropriate distribution on the walls of the retaining forces due to horizontal ties.
4. The values of the reduction factor q are in general slightly higher for stone-masonry systems than for brick-masonry ones in their original configurations. They are always higher than or equal to 1·5, thus exceeding the recommendations of most seismic codes for unreinforced masonry. Strengthenings increased such values, in some instances by a factor up to 1·8 with respect to the original q.
5. The interpretation of recorded signals enabled the description of the change of modal parameters and of energy absorption capacities during strong shocks and the correlation of these changes to the modification of the response mechanism.

ACKNOWLEDGEMENTS

This research was carried out within the Environment CEC research project, funded by the European Community, Contract EV5V-CT92-0174

REFERENCES

1. 'Experimental evaluation of technical interventions to reduce seismic vulnerability of old existing buildings', *Final Report to CEC Environment*, *EV5V-CT92-0174*.
2. D. Benedetti and P. Pezzoli, 'Shaking table tests on masonry buildings. Results and comments', *ISMES – Politecnico di Milano Report*, 1996.
3. P. Carydis, 'Interpretation of the shaking table tests on 12 masonry buildings carried out at LEE', 1996.
4. D. Benedetti and M. P. Limongelli, 'The effect of multi-directional seismic input on determination of modal parameters', in *Structural Dynamics*, *Proc. EURODYN 96*, Balkema, Rotterdam, 1996.
5. W. D. Iwan and A. O. Cifuentes, 'A building for system identification of degrading structures', *Earthquake Engng. Struct. Dyn.* **14**, 877–890 (1986).
6. R. M. Rosemberg, 'The normal modes of nonlinear n-degree-of-freedom systems', *J. Appl. Mech.*, 7–14 (1962).
7. W. D. Iwan and C. Y. Peng, 'An identification methodology for a class of hysteretic structures', *Earthquake Engng. Struct. Dyn.* **21**, 695–712 (1992).

